

## Influence of tropospheric SO<sub>2</sub> emissions on particle formation and the stratospheric humidity

J. Notholt,<sup>1</sup> B. P. Luo,<sup>2</sup> S. Fueglistaler,<sup>3</sup> D. Weisenstein,<sup>4</sup> M. Rex,<sup>5</sup> M. G. Lawrence,<sup>6</sup> H. Bingemer,<sup>7</sup> I. Wohltmann,<sup>5</sup> T. Corti,<sup>2</sup> T. Warneke,<sup>1</sup> R. von Kuhlmann,<sup>6</sup> and T. Peter<sup>2</sup>

Received 3 December 2004; revised 5 March 2005; accepted 15 March 2005; published 9 April 2005.

[1] Stratospheric water vapor plays an important role in the chemistry and radiation budget of the stratosphere. Throughout the last decades stratospheric water vapor levels have increased and several processes have been suggested to contribute to this trend. Here we present a mechanism that would link increasing anthropogenic SO<sub>2</sub> emissions in southern and eastern Asia with an increase in stratospheric water. Trajectory studies and model simulations suggest that the SO<sub>2</sub> increase results in the formation of more sulfuric acid aerosol particles in the upper tropical troposphere. As a consequence, more ice crystals of smaller size are formed in the tropical tropopause, which are lifted into the stratosphere more readily. Our model calculations suggest that such a mechanism could increase the amount of water that entered the stratosphere in the condensed phase by up to 0.5 ppmv from 1950–2000. **Citation:** Notholt, J., et al. (2005), Influence of tropospheric SO<sub>2</sub> emissions on particle formation and the stratospheric humidity, *Geophys. Res. Lett.*, 32, L07810, doi:10.1029/2004GL022159.

### 1. Introduction

[2] Sources of water in the stratosphere are in-situ production resulting from the oxidation of methane and direct transport of water from the troposphere into the stratosphere. Part of the increase of stratospheric water is due to the positive trend of methane emissions, but the magnitude of the observed trend in stratospheric waters is currently still not understood [Oltmans and Hoffmann, 1995; Kley et al., 2000]. Troposphere-to-stratosphere transport of water occurs mainly in the tropics [Holton et al., 1995] in a region termed the Tropical Tropopause Layer (TTL) [Sherwood and Dessler, 2000]. Temperatures around the tropical tropopause are extremely low, resulting in low equilibrium water vapor pressures over ice. The formation of cirrus clouds and sedimentation of ice crystals results in dehydration of air masses as they ascend through this layer.

The total water content of air parcels entering the stratosphere is the sum of gas phase water and water in particles that are too small to sediment efficiently during transport into the stratosphere.

[3] A major source of aerosols in the TTL is the reaction of SO<sub>2</sub> with OH [Brock et al., 1995; Lee et al., 2003] yielding H<sub>2</sub>SO<sub>4</sub>, which subsequently condenses onto existing particles or nucleates with water to form new nanometer sized particles. On a mass basis, other sources of nuclei, such as organic species, condensed meteoric vapor, or particulate matter from aircraft emissions play a smaller role in the TTL [Murphy et al., 1998]. Hence, the number density of aerosols at the dehydration point is strongly influenced by the concentrations of SO<sub>2</sub> and OH in the TTL. Currently about 90% of the SO<sub>2</sub> in the TTL is emitted from the continents, most of the rest is produced by the oxidation of dimethyl sulfide (DMS) of natural marine origin [Thornton et al., 1997]. As we will show, the emissions of SO<sub>2</sub> determine the number concentration and size distribution of aerosols in the TTL. Changes in aerosol number and size will have an impact on the number and size of ice particles, and thus the amount of water transported into the stratosphere as ice crystals.

[4] While anthropogenic SO<sub>2</sub> emissions in Europe and North America have been decreasing since around 1980, the anthropogenic SO<sub>2</sub> emissions from China, Asia and the tropics have been increasing [Streets et al., 2000; van Aardenne et al., 2001; Stern, 2003]. For example, van Aardenne et al. [2001] reports a factor of 12 increase for China and 8 for East Asia, respectively between 1950 and 1990.

[5] We have studied the effect of growing SO<sub>2</sub> emissions from China, Asia and the tropics on the ice water content of TTL air transported into the stratosphere. The simulations were performed in four steps: (i) finding the source regions of airmasses in the TTL (ii) calculation of the number of aerosols formed from SO<sub>2</sub> in the TTL; (iii) calculation of number densities and size distributions of ice crystals; and (iv) estimation of the ice crystal transport into the stratosphere during troposphere-to-stratosphere transport.

### 2. Methods and Results

#### 2.1. Determination of the Source Regions

[6] Very little is known about SO<sub>2</sub> at the tropical tropopause and nothing is known about its trends there. We determine SO<sub>2</sub> concentrations in the TTL by the geographical distribution of emissions at the ground times the probability of the emissions reaching the TTL. We have performed comprehensive trajectory studies to determine the geographical distribution of the origin of air masses in

<sup>1</sup>Fachbereich Physik, Universität Bremen, Bremen, Germany.

<sup>2</sup>Institute for Atmospheric and Climate Science, Eidgenössische Technische Hochschule, Zurich, Switzerland.

<sup>3</sup>Department of Atmospheric Science, University of Washington, Seattle, Washington, USA.

<sup>4</sup>Atmospheric and Environmental Research, Cambridge, Massachusetts, USA.

<sup>5</sup>Alfred Wegener Institute for Polar and Marine Research, Potsdam, Germany.

<sup>6</sup>Max Planck Institute for Chemistry, Mainz, Germany.

<sup>7</sup>Institut für Meteorologie und Geophysik, Johann Wolfgang Goethe Universität, Frankfurt am Main, Germany.

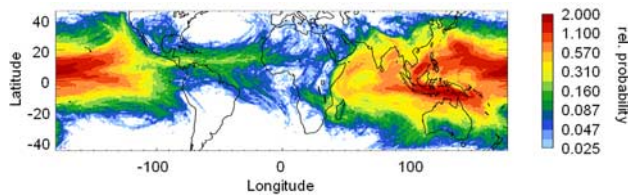


**Figure 1.** Spatial distribution of the probability that lower tropospheric air masses from a given location reach the 380 K isentropic surface.

the TTL (Figure 1). Trajectories have been calculated backwards for up to two months in length, starting at 380 K, i.e. at approximately the tropical tropopause, every 1° in longitude and latitude between 30°S and 30°N. The calculations were based on ECMWF analysis wind fields for two seasons (January/February and July/August), yielding a total of  $2 \times 21960$  trajectories. Because the lifetime of SO<sub>2</sub> is about 100 days in the TTL region and as short as 10 days in the lower troposphere, we limited the time span of the trajectories in the upper troposphere to two months and followed them in the lower troposphere ( $p > 500$  hPa) for two weeks. Figure 1 shows the map of the probability that air masses (trajectories) have been at a given location in the lower troposphere ( $p > 500$  hPa) up to two months prior to observation in the TTL. The number of trajectories that passed through a grid cell were counted and divided by the total number of trajectories, whereby trajectories passing the same grid cell multiple times were counted only once. The figure shows that most of the air masses in the TTL can be traced back to the lower troposphere over Oceania, East Asia, China and India. Calculations with trajectories started at 370 K (not shown) yield very similar results, which demonstrates that the spatial patterns in Figure 1 do not critically depend on the starting level within the TTL. These results have to be interpreted considering the geographical emission patterns. Since emissions in Oceania are small, the SO<sub>2</sub> budget in the TTL is likely dominated by emissions from China and some contributions from East Asia and India. SO<sub>2</sub> emissions from Europe and the Americas play a secondary role as these air masses apparently rarely reach the TTL on the relevant timescales for SO<sub>2</sub>. Our studies are consistent with measurements [Thornton *et al.*, 1997] and trajectory calculations [Folkins *et al.*, 1997], which show that air masses from China, Asia and the tropical belt often reach the tropical Pacific, where they may be lifted into the TTL.

## 2.2. Calculation of Aerosols in TTL

[7] We used a 2-D sulfate aerosol model [Weissenstein *et al.*, 1997] to calculate the number and size distribution of aqueous H<sub>2</sub>SO<sub>4</sub> aerosols formed in the atmosphere. The precursor gases considered are SO<sub>2</sub>, OCS, DMS, H<sub>2</sub>S and CS<sub>2</sub>. The microphysical processes simulated are homogeneous nucleation, condensation and evaporation, coagulation, and sedimentation. Particulate sulfate is treated by size, using 40 bins to cover the size range from 0.39 nm to 3.2 μm in radius by volume doubling. The OH-fields used in the simulations have been calculated with the 3-D chemistry-transport model MATCH-MPIC [Lawrence *et al.*, 2001]. Despite the simplicity of our 2-D model, the results have

been found to be in reasonable agreement with calculations from 3-D models [Pitari *et al.*, 2002] and with PEM tropics data at 10–12 km [Thornton *et al.*, 1999]. The VMR of SO<sub>2</sub> in the TTL was calculated for current conditions. For conditions appropriate to other years, the SO<sub>2</sub> VMR in the TTL was scaled according to the estimated emissions of the source regions China, East Asia, India and Oceania. The main biogenic source of SO<sub>2</sub> in the TTL is due to DMS, which currently contributes less than 10% to the overall SO<sub>2</sub> concentrations in the TTL, as measured by Thornton *et al.* [1997]. We have assumed this natural SO<sub>2</sub> contribution to be constant. We find that the number and size of H<sub>2</sub>SO<sub>4</sub>/H<sub>2</sub>O particles in the TTL depend directly on the SO<sub>2</sub> concentrations. Changes in SO<sub>2</sub> lead to changes in the nucleation and condensation of the aqueous sulfuric acid droplets. Nucleation and coagulation both control particle numbers, condensation and coagulation both control their size distribution. For the situation of 1950 for example, with emissions of 17% of the present, the resulting particle number concentration is 25% of its current value.

## 2.3. Calculation of Ice Crystals

[8] Upon ascending and cooling to temperatures below the frost point, a fraction of the aerosols serve as condensation nuclei to form ice crystals, depending entirely on the H<sub>2</sub>SO<sub>4</sub>/H<sub>2</sub>O particle distribution calculated in (ii) and on the mesoscale temperature fluctuations at the time of ice nucleation. We use a microphysical model to calculate the number concentration and size of the ice crystals formed [Hoyle *et al.*, 2005], assuming homogeneous freezing of the H<sub>2</sub>SO<sub>4</sub>/H<sub>2</sub>O aerosol droplets. The final ice number density of the cirrus clouds depends both on the aerosol loading and the cooling rate in the moment of the nucleation, which is dominated mainly by the mesoscale gravity wave activities

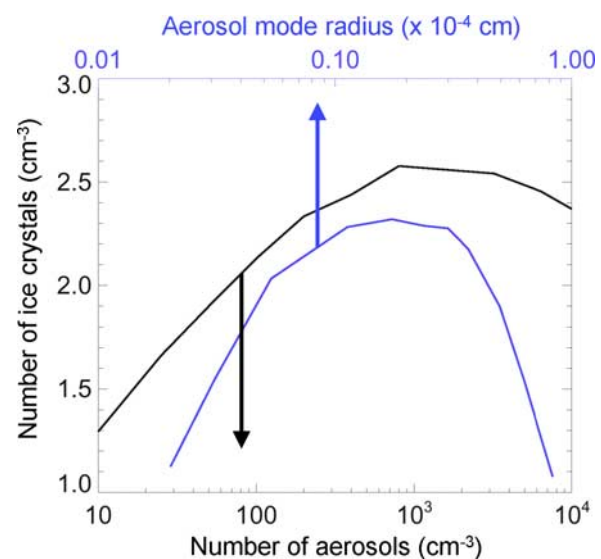


**Figure 2.** Ice number density as a function of the total number density of aerosol with a fixed mode radius of 0.1 μm (black curve) or as a function of the mode radius with a fixed number density of 100 cm<sup>-3</sup> (blue curve) during a cooling event with a cooling rate of 10 K h<sup>-1</sup>. A lognormal aerosol distribution is used for the entire simulation with  $\sigma = 1.2$  and a freezing temperature of  $\sim 192$  K.

(except in strong convection channels). The distribution of the cooling rates is based on aircraft measurements of vertical wind during the SUCCESS campaign [Hoyle *et al.*, 2005]. The temperature fluctuations lead to relatively high ice number densities, which deplete the gas phase to values close to the equilibrium vapor pressure over ice.

[9] First, the ice number density of a cirrus cloud formed from nucleation onto aqueous sulfuric acid droplets during a cooling event depends on the cooling rate. At higher cooling rates, higher supersaturations can be reached, and more ice particles can be formed. Secondly, the number of ice crystals formed during a cooling event depends also on the size and number density of the aerosols, Figure 2. For a fixed median aerosol size the number density of ice crystals increases with the number of aerosols, until the total number density exceeds  $1000\text{ cm}^{-3}$ . Increases in aerosol particle size also cause similar increases in ice number density unless the particle size is greater than  $0.2\text{ }\mu\text{m}$ . This last fact results from the Kelvin effect. Since smaller particles have a higher vapor pressure they are more concentrated in sulfuric acid, which leads to a smaller nucleation coefficient. Therefore, aerosol particles will be activated successively upon cooling, depending on their size. An aerosol particle distribution of smaller size shows a larger range in nucleation temperatures compared to an aerosol particle distribution of larger size. Therefore as the median size increases a larger fraction of particles will nucleate at a fixed supersaturation leading to more ice, whereas as median size decreases the fraction which nucleates will decrease, the larger particles which do nucleate will deplete the gas phase lowering the supersaturation.

[10] In the case of interest here, the aerosol particle concentration and size are always below the limits of  $1000\text{ cm}^{-3}$  and  $0.2\text{ }\mu\text{m}$ . Therefore the increased SO<sub>2</sub> will always lead to more ice particles nucleating homogeneously, irrespective whether the underlying aerosol distribution is higher in number density or larger in size. For the situation of 1950 for example, the ice crystal number density is reduced to approximately 70% of the value for 2000.

#### 2.4. Transport of Ice Crystals Into Stratosphere

[11] Several mechanisms have been proposed to be responsible for the final dehydration of air entering the stratosphere [Sherwood and Dessler, 2000]: gradual ascent, horizontal advection in regions where the tropopause intersects the isentropic surfaces, deep convection, or dehydration during adiabatic cooling in a wave event. In order to precisely calculate the amount of condensed phase that enters the stratosphere, a highly detailed cloud model [e.g., Jensen and Pfister, 2004] would have to be applied/used. Here, we employ a much simpler calculation to evaluate the sensitivity of stratospheric water vapor mixing ratios to a systematic decrease in ice particle size in cirrus in the TTL. In particular, we focus on the order of magnitude of the change in the amount of water entering the stratosphere in the condensed phase between 1950 and 2000.

[12] The transport of the ice crystals by gradual ascent has been calculated by convolving the sedimentation velocity distribution of the particles with the vertical upward velocity distribution in the TTL (Figure 3). The probability distribution of the diabatic component of the vertical wind field was derived from 1 day forward trajectories calculated

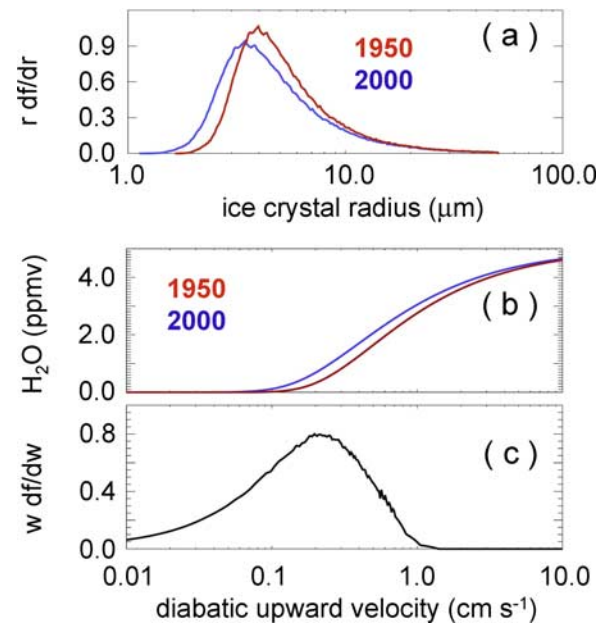


**Figure 3.** (a) Ice crystal radius distributions calculated from the cooling rate distribution deduced from aircraft measurements of vertical winds during the SUCCESS campaign. Blue line: SO<sub>2</sub> in 2000; red line: SO<sub>2</sub> reduced to 1950s loading. (b) Amount of particulate water transported into the stratosphere as a function of the vertical velocity of an air parcel undergoing gradual ascent. Blue line: for the SO<sub>2</sub> loading in 2000; red line: SO<sub>2</sub> reduced to 17%, corresponding to the 1950s loading. The calculation of the ice crystals has been performed for an ice water content of 5 ppmv. (c) Distribution of large scale upwelling velocity derived from heating rates based on ECMWF analyses at  $\theta = 370\text{ K}$  in the tropics between  $20^{\circ}\text{S}$  and  $20^{\circ}\text{N}$  for the periods January/February, and July/August 2001 combined.

from ECMWF analysis data [Fueglistaler *et al.*, 2004]. While the total amount of condensed phase water that enters the stratosphere depends strongly on the assumptions on the diabatic lifting, the differential effect due to changes in SO<sub>2</sub> between 1950 and 2000 is similar for the various vertical velocity scenarios. On the average we calculate an increase in the stratospheric humidity of 0.5 ppmv between 1950 and 2000. If the vertical velocities were changed by  $\pm 20\%$ , the calculated increase in the stratospheric humidity between 1950 and 2000 changes by  $\pm 5\%$ ; changes of  $\pm 50\%$  in the diabatic uplift changes the increase between 1950 and 2000 by  $\pm 20\%$ . The variability of  $\pm 50\%$  for the diabatic uplift is a plausible range for its uncertainties.

[13] In order to cover also the other dehydration mechanisms we have developed a more general model based on a Lagrangian perspective, where the transport of ice into the stratosphere is estimated from incomplete dehydration due to the limited 'cloud lifetime' (i.e. not all ice crystals have enough time to sediment out of the corresponding air mass). In this way the model is applicable to gradual ascent, horizontal advection and adiabatic cooling. Using realistic values for the vertical thickness of thin cirrus at the tropical tropopause (several hundreds of meters) and cloud lifetime (a few hours to 1–2 days), in combination with our

calculated ice particle size distribution, yields results very similar to the calculations shown above.

### 3. Discussion and Conclusions

[14] The mechanism presented here applies to air masses that enter the stratosphere through slow radiatively driven ascent and should not be confused with a similar mechanism proposed by *Sherwood* [2002] for ice particles that form in convective events and enter the stratosphere in convective overshoot.

[15] A few observations of thin cirrus clouds in the tropics exist supporting our mechanism proposed [*Winker and Trepte*, 1998; *Pfister et al.*, 2001; *Santacesaria et al.*, 2003]. Furthermore isotopic studies by *Webster and Heymsfield* [2003] show that 25% of lower stratospheric water originates from ice evaporation, supporting the view that transport of particulate water is indeed relevant for stratospheric humidity.

[16] Besides aerosols from SO<sub>2</sub>, biomass burning aerosols [*Sherwood*, 2002], sea salt aerosols, meteoric aerosols, and desert dust serve as condensation nuclei for cirrus clouds [*Cziczo et al.*, 2004]. Including these other condensation nuclei will increase the total number of condensation nuclei in the TTL. However, our calculations show that even when increasing the number density of the baseline background aerosols in 2000 by up to a factor of five, the SO<sub>2</sub> increase between 1950 and 2000 still leads to an increase of water transported into the stratosphere.

[17] Our mechanism suggests that SO<sub>2</sub> emissions in China and South and East Asia have an influence on the stratospheric humidity, inducing a multi-decadal trend on top of the observed interannual variability [*Randel et al.*, 2004], largely driven by the variability in temperature. We compute that the SO<sub>2</sub> increase since the 1950s in China and South and East Asia may have led to an increase of up to 0.5ppmv in stratospheric water, which could in part account for the observations [*Oltmans and Hoffmann*, 1995; *Kley et al.*, 2000; *Randel et al.*, 2004]. The Pinatubo eruption in June 1991 greatly perturbed the composition of the stratosphere, and perhaps of the TTL. This might also influence the stratospheric humidity in a way suggested by our process, but changes in temperature induced by the Pinatubo eruption likely dominate the overall effect on the stratospheric humidity.

[18] **Acknowledgments.** We would like to thank MeteoSwiss for providing the ECMWF data. This work was performed within the SPARC Aerosol Assessment. Work at AER was funded by the NASA Atmospheric Chemistry Modeling and Analysis Program.

### References

Brock, C. A., P. Hamill, J. C. Wilson, H. H. Jonsson, and K. R. Chan (1995), Particle formation in the upper tropical troposphere: A source of nuclei for the stratospheric aerosol, *Science*, *270*, 1650–1653.

Cziczo, D. J., D. M. Murphy, P. K. Hudson, and D. S. Thomson (2004), Single particle measurements of the chemical composition of cirrus ice residue during CRYSTAL-FACE, *J. Geophys. Res.*, *109*, D04201, doi:10.1029/2003JD004032.

Folkens, I., R. Chatfield, D. Baumgardner, and M. Proffitt (1997), Biomass burning and deep convection in southeastern Asia: Results from ASHOE/MAESA, *J. Geophys. Res.*, *102*, 13,291–13,299.

Fueglistaler, S., H. Wernli, and T. Peter (2004), Tropical troposphere-to-stratosphere transport inferred from trajectory calculations, *J. Geophys. Res.*, *109*, D03108, doi:10.1029/2003JD004069.

Holton, J. R., P. H. Haynes, M. E. McIntyre, A. R. Douglas, D. B. Rood, and L. Pfister (1995), Stratosphere-troposphere exchange, *Rev. Geophys.*, *33*, 403–440.

Hoyle, C. R., B. P. Luo, and T. Peter (2005), The origin of high ice crystal number densities in cirrus clouds, *J. Atmos. Sci.*, in press.

Jensen, E., and L. Pfister (2004), Transport and freeze-drying in the tropical tropopause layer, *J. Geophys. Res.*, *109*, D02207, doi:10.1029/2003JD004022.

Kley, D., J. M. Russell III, and C. Phillips (2000), SPARC Assessment of upper tropospheric and stratospheric water vapour, *WCRP-113, WMO/TD-No. 1043*, World Meteorol. Org., Geneva.

Lawrence, M. G., P. Jöckel, and R. von Kuhlmann (2001), What does the global mean OH concentration tell us?, *Atmos. Chem. Phys.*, *1*, 37–49.

Lee, S.-H., J. M. Reeves, J. C. Wilson, D. E. Hunton, A. A. Viggiano, T. M. Miller, J. O. Ballenthin, and L. R. Lait (2003), Particle formation by ion nucleation in the upper troposphere and lower stratosphere, *Science*, *301*, 1886–1889.

Murphy, D. M., D. S. Thomson, and M. J. Mahoney (1998), In situ measurements of organics, meteoritic material, mercury, and other elements in aerosols at 5 to 19 kilometers, *Science*, *282*, 1664–1669.

Oltmans, S. J., and D. J. Hoffmann (1995), Increase in lower-stratospheric water vapour at a mid-latitude Northern Hemisphere site from 1981 to 1994, *Nature*, *374*, 146–148.

Pfister, L., et al. (2001), Aircraft observations of thin cirrus clouds near the tropical tropopause, *J. Geophys. Res.*, *106*, 9765–9786.

Pitari, G., E. Mancini, V. Rizi, and D. T. Shindell (2002), Impact of future climate and emission changes on stratospheric aerosols and ozone, *J. Atmos. Sci.*, *59*, 414–440.

Randel, W. J., F. Wu, S. J. Oltmans, K. Rosenlof, and G. E. Nedoluha (2004), Interannual changes of stratospheric water vapor and correlations with tropical tropopause temperatures, *J. Atmos. Sci.*, *61*, 2133–2148.

Santacesaria, V., et al. (2003), Clouds at the tropical tropopause: A case study during the APE-THESIO campaign over the western Indian Ocean, *J. Geophys. Res.*, *108*(D2), 4044, doi:10.1029/2002JD002166.

Sherwood, S. (2002), A microphysical connection among biomass burning, cumulus clouds, and stratospheric moisture, *Science*, *295*, 1272–1275.

Sherwood, S., and A. Dessler (2000), On the control of stratospheric humidity, *Geophys. Res. Lett.*, *27*, 2513–2516.

Stern, D. I. (2003), Global sulfur emissions in the 1990s, *Rensselaer Working Pap. Econ. 0311*, 33 pp., Rensselaer Polytech. Inst., Troy, N. Y.

Streets, D. G., N. Y. Tsai, H. Akimoto, and K. Oka (2000), Sulfur dioxide emissions in Asia in the period 1985–1997, *Atmos. Environ.*, *34*, 4413–4424.

Thornton, D. C., A. R. Bandy, B. W. Blomquist, J. D. Bradshaw, and D. R. Blake (1997), Vertical transport of sulfur dioxide and dimethyl sulfide in deep convection and its role in new particle formation, *J. Geophys. Res.*, *102*, 28,501–28,510.

Thornton, D. C., A. R. Bandy, B. W. Blomquist, A. R. Driedger, and T. P. Wade (1999), Sulfur dioxide distribution over the Pacific Ocean 1991–1996, *J. Geophys. Res.*, *104*, 5845–5854.

van Aardenne, J. A., F. J. Dentener, J. G. J. Olivier, C. G. M. Klein Goldewijk, and J. Lelieveld (2001), A 1° × 1° resolution data set of historical anthropogenic trace gas emissions for the period 1890–1990, *Global Biogeochem. Cycles*, *15*, 909–928.

Webster, C., and A. J. Heymsfield (2003), Water isotope ratios D/H, <sup>18</sup>O/<sup>16</sup>O, <sup>17</sup>O/<sup>16</sup>O in and out of clouds map dehydration pathways, *Science*, *302*, 1742–1745.

Weisenstein, D. K., G. K. Yue, M. K. W. Ko, N.-D. Sze, J. M. Rodriguez, and C. J. Scott (1997), A two-dimensional model of sulfur species and aerosols, *J. Geophys. Res.*, *102*, 13,019–13,036.

Winker, D. M., and C. R. Trepte (1998), Lamina cirrus observed near the tropical tropopause by LITE, *Geophys. Res. Lett.*, *25*, 3351–3354.

H. Bingemer, Institut für Meteorologie und Geophysik, Johann Wolfgang Goethe Universität, D-60325 Frankfurt am Main, Germany.

T. Corti, B. P. Luo, and T. Peter, Institute for Atmospheric and Climate Science, Eidgenössische Technische Hochschule, CH-8093 Zurich, Switzerland.

S. Fueglistaler, Department of Atmospheric Science, University of Washington, Seattle, WA 98195, USA.

M. G. Lawrence and R. von Kuhlmann, Max Planck Institute for Chemistry, D-55020 Mainz, Germany.

J. Notholt and T. Warneke, Fachbereich Physik, Universität Bremen, D-28334 Bremen, Germany. (notholt@uni-bremen.de)

M. Rex and I. Wohltmann, Alfred Wegener Institute for Polar and Marine Research, D-14473 Potsdam, Germany.

D. Weisenstein, Atmospheric and Environmental Research, Cambridge, MA 02139–3794, USA.